

Numerical Method for Predicting the Sound Reduction Index of a Double Panel Including an Active Control System and Porous Material

Azzedine Sitel, Catherine Guigou-Carter, Philippe Jean

CSTB, Center for Building Science and Technology, 24 Rue Joseph Fourier 38400 Saint Martin d'Hères, France.
Azzedine.sitel@free.fr

Summary

In this paper, a numerical method for predicting the sound reduction index of a double wall including an active control system and a porous layer inside the double wall cavity is presented. The double wall is placed in a laboratory situation between an emission and a reception room. Active control sources and error microphones are distributed in two vertical planes located inside the double wall cavity. The secondary sources role is to improve the sound reduction index at low frequencies by reducing the acoustical pressure at microphone positions created by the primary source placed inside the emission room. The simulation principle is based on the decoupled Green method where the radiated pressure inside the reception room is deduced from the double wall velocity and from the reception room Green's functions. The double wall and the active control system are modelled by finite element method using Nastran software. The two rooms Green's functions are analytically modelled using a modal method. The model allows investigating effects of various parameters on active control efficiency, such as the effect of evanescent modes inside the double wall cavity, the double wall cavity thickness, the number of control channels as well as the effect of a porous layer inserted inside the double wall cavity placed between secondary sources plane and error microphones plane.

PACS no. 43.40.Rj, 43.50.Gf, 43.50.Ki, 43.55.Br, 43.55.Ka, 43.55.Ti, 43.55.Vi

1. Introduction

Most of new buildings are equipped with gypsum board partition walls involving one or more layers of air or absorbing material which are responsible for a vibroacoustic coupling between successive sheets. Such layered walls are very efficient in terms of the sound insulation, except at the lower frequencies especially when walls resonances occur [1, 2, 3, 4, 5, 6]. To get high acoustic insulation at low frequencies, such walls should require an unacceptable quantity of materials (i.e. adding mass, increasing cavity thickness, etc...). As there is a few hope of increasing significantly the performances of passive materials at low frequencies, active control has been investigated in previous works [3, 4, 5, 6] as an alternative to improve double wall sound insulation at low frequencies. This paper presents a numerical method for predicting the sound reduction index of a double panel equipped with active control sources. The double panel separates an emission and a reception room and is composed of two gypsum plates sandwiching an air cavity. In this first approach the metallic frame on which the gypsum boards are usually

mounted on, is not taken into account. The panel is excited by an acoustic field generated by an acoustic source (monopole) placed in the corner of the emission room. In order to improve by active noise control the transmission loss of the double panel at low frequencies, N secondary sources (monopoles) are distributed on a vertical plane area located in the air cavity coupling the two plates. The complex amplitude spectrum of each monopole is introduced in the calculations so that the pressure level is minimized at error microphones positions.

It should be noted that even at low frequencies, the (sound insulation performances) / (cost, mass and thickness) ratio of the active double wall studied in this paper remains too low in comparison with that of most passive partitions used in buildings or transport industry. This is all the more true as standard loudspeakers are used as noise control sources making active control hardware heavy, expensive and bulky. However, due to recent developments in digital electronic technology and due to the rapid technology growth in other fields, it is nowadays technically possible to develop lightweight loudspeakers (i.e. piezoelectric loudspeakers [4, 5, 6], ultra-thin flat, flexible loudspeaker (FFL) [7], etc...) as well as efficient and miniature electronic controllers. This would make active noise control hardware lightweight and not bulky. Furthermore, in the upcoming years, eventual production and commer-

cialization of active noise control technology on a large-scale would certainly make active control solutions affordable and more advantageous compared to some passive solutions. The focus of this work is to simulate and discuss, independently of technical considerations, physical mechanisms and the associated advantages and limitations occurring when an active noise control system is mounted inside a small thickness air cavity coupling two plates. Indeed, when lateral dimensions of the double panel are not too small with respect to the wavelength, higher acoustical modes propagate even at very low frequencies making the acoustical field very complex in the air cavity [8, 9, 10, 11]. Consequently, the attenuation by active control of the acoustic pressure at some points of a vertical surface located inside the cavity, can not inevitably reduce the global acoustical field in this entire surface. This makes global noise control extremely difficult. The interest of this study is to bring a best understanding about difficulties and limits related to this active noise control system. Also, simulations presented here will enable to check effects of some solutions proposed to improve the active control efficiency such as increasing the number of control channels or inserting a porous layer between secondary sources plane and error microphones plane. The numerical model is based on the decoupled GRIM method previously developed for modelling passive walls [12, 13, 14]. The double panel and secondary sources are modelled by finite element method using Patran/Nastran software. The acoustic field in the reception room is computed from an integral method using the receiving room Green's functions [12].

In this paper a description of the GRIM approach is given first. Then, a simulation method of the sound reduction index in the case of active noise control is described and effects of some parameters on active control efficiency such as evanescent modes inside the double wall cavity, the cavity thickness, the number of control channels are presented and discussed. The effect of a porous layer inserted between secondary sources plane and error microphones plane is also investigated.

2. Description of the GRIM approach

Consider a partition separating an emission and a reception rooms as shown in Figure 1. The emission room is excited by an acoustic source placed in one corner. In order to model the sound reduction index of partitions in buildings range from very simple (plain concrete wall) to complex structures (double walls, bricks, hollow core slabs...), a simulation method has been developed by CSTB under the acronym GRIM (green ray integral method [12, 13, 14]). The principle is based on a decoupled model for sound transmission problems. The radiated pressure P_r at a point M in the reception room is evaluated as

$$P_r(M) = -j\omega \int_{S_2} V_2(Q) G_2(M, Q) dS(Q), \quad (1)$$

where S_2 is the radiating surface of the partition located at z_r , V_2 is the velocity of the partition at a point Q of the

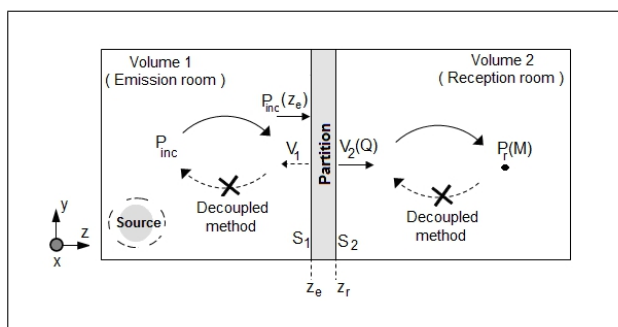


Figure 1. Decoupled sound transmission between two volumes 1 and 2 separated by a partition of boundaries S_1 and S_2 .

surface S_2 . G_2 is the Green function in the reception room computed for the vibrating wall considered to be motionless but keeping all other acoustical boundaries unchanged [12]. The computation of the velocity V_2 at the radiating surface S_2 is carried out by modelling the partition with commercial software NASTRAN based on finite element method. This allows the consideration of complex walls with practical boundary conditions. The load or the excitation for Nastran input file is here the incident pressure P_{inc} applied at the receiving surface S_1 of the partition. P_{inc} is deduced from the Green function G_1 in the emission room. According to the studied frequency range and rooms properties (dimensions, geometry, walls absorption coefficient), Green functions G_1 and G_2 can be computed by different means such as modal approaches, BEM or geometrical models [15, 16]. In this work, Green functions G_1 and G_2 are analytically computed using the modal approach [12] because the modal density in the two rooms is not very high in the studied frequency range. With this decoupled GRIM approach, the vibroacoustic coupling between the two rooms and the partition is not fully considered. In fact, effect of the pressure P_r on the velocity V_2 and effect of the velocity V_1 on the pressure P_{inc} are not taken into account (see Figure 1). Solving the fully coupled problem is quite possible [1] but is computationally expensive. In many cases, the consideration of full coupling is not necessary. Modal approaches, based on coupled or decoupled models, may give almost identical results in the case of sound transmission between two rooms [13]. Full coupling is however, necessary for small volumes such as air gaps between double glazings [17].

The sound reduction index $R(dB)$ is evaluated from the ratio between incident and radiated acoustic powers,

$$R(dB) = 10 \log (W_{inc}/W_r). \quad (2)$$

Incident and radiated power W_{inc} and W_r are deduced from the mean square pressure in the emission and the receiving rooms [12]. Results here presented have been obtained by using the computer program named GAIA [13] which can be employed for the computation of acoustic pressures P_r and P_{inc} in each point of the emission and the reception rooms.

3. Simulation of the sound reduction index in the case of active noise control

Consider a double panel separating two rooms as shown in Figure 2. N active control sources are distributed inside the double panel air cavity in a vertical plane located at z_s . Each secondary source is associated to one error microphone located in microphones plane at z_m . The double panel is excited by an acoustic field generated by a primary source placed in the corner of the emission room. The role of secondary sources is to improve the sound reduction index R by cancelling the acoustic pressure at microphone positions created by the primary source placed in the emission room. In this work, secondary or control sources are modelled as monopole sources. In the case of active control, the sound reduction index is simulated through two main steps:

- The first step is the optimization of secondary sources (monopoles) by computing their complex amplitude spectrum enabling to cancel the acoustic pressure at error microphones positions.
- The second step involves the computation of the transmitted field resulting from the action of the primary source placed in the emission room and the N secondary sources (monopoles with optimized complex amplitude spectrum) located inside the cavity of the double panel.

3.1. Secondary sources optimization procedure

In the case of N secondary sources and N error microphones, the complex amplitude spectrum of secondary sources enabling the cancellation of the acoustic pressure at error microphones positions are deduced as [3]

$$\{A_j^{Sc}\}_{1 \times N} = [B]_{N \times N}^{-1} \times \{P^{pri}\}_{N \times 1}. \quad (3)$$

$[B]_{N \times N}$ is the secondary path matrix. A column j of $[B]_{N \times N}$ is filled with terms B_{ij} which represent the complex amplitude pressure spectrum at the i th error microphone caused by the j th secondary source having a unit amplitude for all frequencies. $\{P^{pri}\}_{N \times 1}$ is the primary source vector whose N terms represent the acoustic pressure spectrums at the N error microphone positions created by the primary source located in the emission room. In order to optimize secondary sources, we have to determine the N columns of the matrix $[B]_{N \times N}$ as well as the vector $\{P^{pri}\}_{N \times 1}$. The optimization procedure of secondary sources is achieved into 6 steps which are listed below and graphically depicted in Figure 3:

1. Firstly, the pressure field distribution in the emission room is computed with GAIA program at all nodes of a regular grid located on the excited surface S_1 of the partition. A file named PRESS is then created, it contains the incident pressure spectrum $P_{inc}(x_i, y_j, z_e, f)$ at all nodes of the regular grid.
2. A FEM meshing of the partition (double panel including its acoustic cavity) is realized with PATRAN which is the standard mesher associated with NASTRAN software (commercial solver based on FEM). The output is

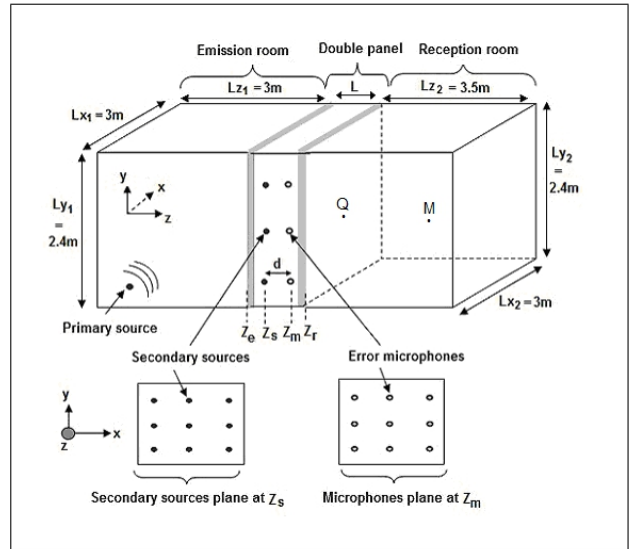


Figure 2. Active double wall including 9 control channels separating an emission and a reception rooms.

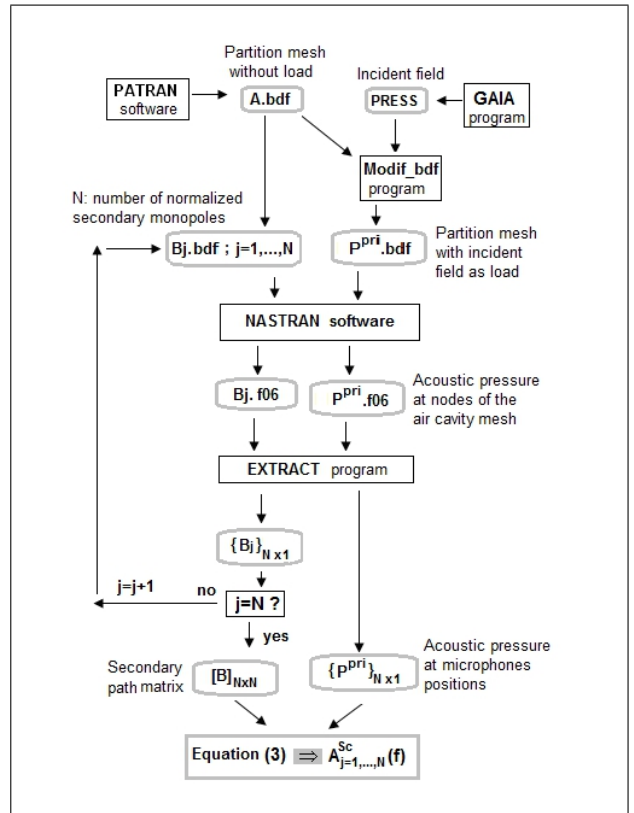


Figure 3. Flow chart describing optimization steps of the amplitude spectrum of secondary sources.

(A.bdf) file which is the input file to NASTRAN. At this stage, the excitation (load) is not yet implemented in (A.bdf) file.

3. $N + 1$ different files (.bdf) are then generated from A.bdf. The first one is associated to the primary source. To do this, an input interface program (Modif_bdf) was written to include the PRESS file into the file (A.bdf) under the form of a distributed pressure spec-

trum $P_{inc}(x_i, y_j, z_e, f)$. This results in a new bdf file ($P^{pri}.bdf$). Each one of the N other files ($B_{j=1, \dots, N}.bdf$) corresponds to one secondary source monopole excitation placed at the associated node of the air cavity mesh. At this stage, all control source monopoles have unit amplitude over the frequency range selected.

4. FEM solver software NASTRAN is then run once with the input file $P^{pri}.bdf$, and then N times with input files ($B_{j=1, \dots, N}.bdf$). Outputs are $N + 1$ files ($B_{j=1, \dots, N}.f06$) and ($P^{pri}.f06$) containing the acoustical pressure spectrum at all mesh nodes of the air cavity coupling the two plates.
5. The acoustic pressure spectrum at mesh nodes corresponding to the N error microphones positions is extracted from files ($B_{j=1, \dots, N}.f06$) and ($P^{pri}.f06$). To do this, a program named EXTRACT has been created. Outputs are N vectors $\{B_{j=1, \dots, N}\}_{N \times 1}$ and $\{P^{pri}\}_{N \times 1}$ containing the complex amplitude spectrum of the acoustical pressure at N microphones positions.
6. The last optimization procedure step is to store the N vectors $\{B_{j=1, \dots, N}\}_{N \times 1}$ under the form of the secondary path matrix $[B]_{N \times N}$ and to compute using Equation (3), the amplitude spectrum $A_{j=1, \dots, N}^{Sc}(f)$ for the N control sources enabling the cancellation of the acoustic pressure at N error microphone locations. Outputs are N files, each one is associated to one secondary source monopole containing its optimized complex amplitude spectrum.

3.2. Computation of the sound reduction index in the case of active control

The transmitted acoustic field spectrum P_r into the receiving room resulting from the action of the primary source and the N optimized secondary sources is evaluated following the steps described in Figure 4 and listed below:

1. An input file (D.bdf) for Nastran is created for an excitation combining the primary field $P_{inc}(x_i, y_j, z_e, f)$ and the N control sources with their optimized amplitude $A_{j=1, \dots, N}^{Sc}(f)$. D.bdf is created from ($P^{pri}.bdf$) by introducing N monopole excitations with amplitudes located at nodes corresponding to the N secondary sources positions. This step is carried out thanks to a program named CONTROL (see flow chart of Figure 4).
2. Nastran is run with the input file (D.bdf) and an output file (D.f06) is generated. (D.f06) contains the velocity field at all mesh nodes of the two plates as well as the acoustical velocity at nodes of the air cavity at each frequency considered.
3. A post-treatment program (Vit_Nastran) has been used to extract the velocity spectrum from the output file (D.f06) at radiating nodes (located at S_2) and to store them into a compact binary file (D.vit) of reduced size compared to D.f06.
4. GAIA program is run using the velocities input from file (D.vit). The acoustic pressures P_r in the receiving room is then obtained using equation (1) as well as the incident field P_{inc} inside the emission room. The sound

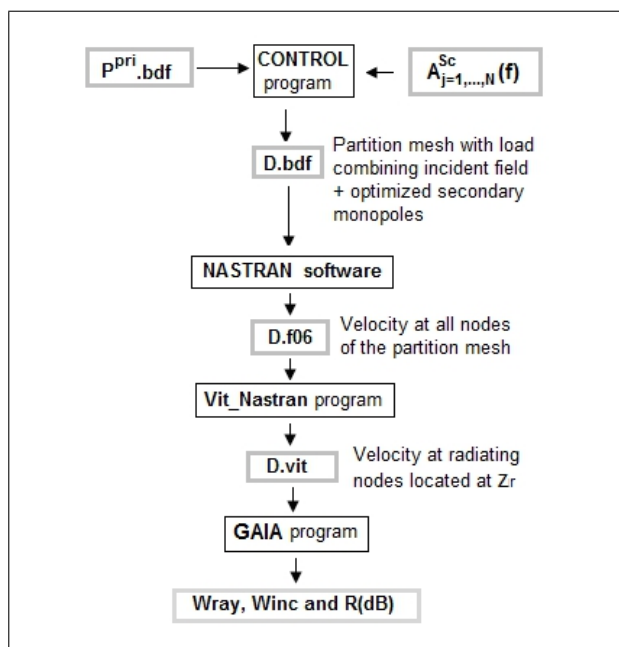


Figure 4. Flow chart describing computation steps of the sound reduction index R in the case of active control.

reduction index $R(dB)$ in the case of active control is finally evaluated from the ratio between incident and radiated acoustic power using equation (2).

4. Results

It should be noted that finite element computation steps involving Nastran software can be achieved by two different methods [18]. The first one is the modal method (modal frequency response analysis corresponding to Nastran solver 111). With this modal method, the solution (acoustic pressure or velocity) at mesh nodes of the partition is computed from acoustical and structural modes. The number of acoustical or structural modes can be fixed in order to reduce the computation time. However, the convergence in terms of number of modes considered must be checked and validated. The second method is the direct method (direct frequency response analysis corresponding to Nastran solver 108), the solution at nodes is exact and all modes are indirectly taken into account in computation. The computation time is therefore more important compared to the modal method. Results presented here are plotted versus frequency, in the range between 20 and 200 Hz. The two partitions are considered identical and lateral walls of the cavity coupling the two plates are assumed rigid. The two partitions are clamped. The double wall cavity is assumed to be filled by air. Physical properties and dimensions of partitions and rooms are listed below in Table I. For all figures, the thickness L of the air cavity is equal to 20 cm and the distance d between error microphones and control sources planes is equal to 10 cm. Finite Element parameters of the partition (gypsum plate /air cavity/ gypsum plate) used during Nastran computation steps are given by Table II.

Table II. Finite Elements parameters of the partition used by Nastran calculations.

	Gypsum plate 1 or 2	Air cavity	Total partition
Type of element	CHEXA	CHEXA	CHEXA
Number of nodes per element	8	8	8
Number of elements	30×24×1	30×24×20	30×24×22
Number of nodes	1550	16275	19375
Minimal wavelength λ_{\min}	>400 cm	172,5 cm	
Number of element per λ_{\min}	>40	17	

Table I. Characteristics and dimensions of investigated double wall and rooms.

Plates of the double wall	
Width	$L_x = 3$ m
Height	$L_y = 2.4$ m
Thickness	$h = 25$ mm
Material	gypsum
Density	$\rho = 725$ kg/m ³
Young's modulus	$E = 0.684$ GPa
Poisson's ratio	$\nu = 0.1$
Loss factor	$\eta' = 0.01$
Boundary conditions	Clamped
Emission and reception rooms	
Width	$L_{x1} = L_{x2} = 3$ m
Height	$L_{y1} = L_{y2} = 2.4$ m
Length	$L_{z1} = 3$ m, $L_{z2} = 3.5$ m
Normal absorption coefficient of walls rooms	$\alpha = 0.4$
Air cavity coupling the two plates	
Density	$\rho_0 = 1.213$ kg/m ³
Speed of sound	$c_0 = 343$ m/s
Thickness	$L = 20$ cm

Table III. Cut-off frequencies of acoustical transverse modes in the double wall air cavity.

(m, n)	f_{mn} : Cut-off frequency (Hz)
(0, 0)	0
(±1, 0)	57.5
(0, ±1)	71.9
(±1, ±1)	92
(±2, 0)	115
(±2, ±1)	135
(0, ±2)	143
(±1, ±2)	154
(±3, 0)	172.5
(±2, ±2)	184
(±3, ±1)	186
(0, ±3)	215

Note that in order to reduce the computation time during FE simulation steps described in Figures 3 and 4, the two gypsum plates have been modelled here with only 1 linear 8-noded HEXA element over the thickness. As the stress/strain information in such elements is given by a constant function, this could add artificial stiffness to the

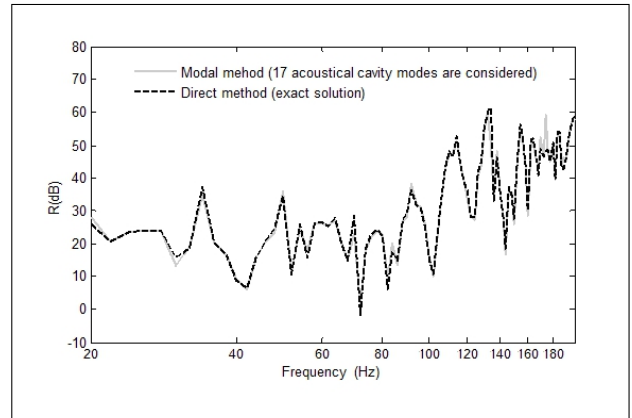


Figure 5. Predicted sound reduction index R (dB) for passive case (without active control).

model. As a rule of thumb one should try to have at least 4 linear elements over the thickness to avoid artificial stiffness.

Figure 5 represents the sound reduction index R for passive case (without active noise control). The grey curve is computed with the modal method where only acoustic modes in cavity whose the cut-off frequency is lower than 150 Hz are considered in computation (see Table III). Note that in order to study the influence of only acoustic modes in the air cavity, a large number of structural modes equal to 349 has been considered by the modal method. The dashed black curve is computed with the direct method (exact solution). With this direct method, all acoustic modes are indirectly considered in calculations even if they are evanescent in the studied frequency range.

As expected, the difference between the two curves is very small specially below 150 Hz. There is almost no influence on the index R of all acoustic modes which are evanescent below 150 Hz and not considered by the modal method. This is in agreement with equation (A10) because the acoustic intensity of evanescent modes is equal to zero (see Appendix). No acoustic energy can therefore be transmitted through evanescent modes from one gypsum plate to the other. We can conclude that for passive case (without active control), effect on the sound reduction index R of evanescent modes in the cavity is negligible.

On the other hand, the global tendency of the curve of the index R is in agreement with previous works [1]. The sound reduction index R decreases at particular frequencies corresponding to plates structural resonances (near

42, 71, 82, 102 and 144 Hz for example). The dip located near 45 Hz is due to the mass-spring-mass resonance of the double panel which is highly depending on the air cavity thickness L .

Figure 6 shows the sound reduction index R computed with and without active control. Active control is simulated in the case of 9 secondary sources and 9 error microphones (spatially distributed as indicated in Figure 2) for pressure cancellation at microphones positions. For the two curves, finite element calculation steps are carried using the direct method (exact solution). Generally, the sound reduction index R simulated with active control is higher than passive one for frequencies below 160 Hz. This is in agreement with the half-wavelength rule [3] since the gain on the index R obtained by active control remains positive below a particular frequency f_{\max} whose the half wavelength λ_{\max} is equal to the distance D between secondary sources,

$$f_{\max} = \frac{c_0}{2D}, \quad (4)$$

where c_0 is the speed of sound in air.

Indeed, for 9 secondary sources and 9 microphones, the distance D is close to 1 m, leading a frequency f_{\max} close to 172 Hz.

However, the gain on the sound reduction index R obtained by active control varies strongly with frequency. Near to 34 Hz, we can notice a striking dip on the curve simulated in active control case. This can be explained by a small pressure level at microphones positions since the index R simulated without active control is relatively high (more than 32 dB) at this frequency. We can also notice an inverse tendency at 41 Hz which can be explained by the high pressure level at error microphones since $R(\text{dB})$ is lower than 10 dB at this frequency.

In order to understand causes of those results, we have plotted in Figure 7 the gain on sound reduction index R obtained by active control which is the difference between $R(\text{dB})$ computed with and without active control. The black curve is simulated with the direct method (exact solution). The dashed grey curve is simulated with the modal method where 33 acoustic modes (representing all cavity modes presented in Table III, i.e. all cavity modes up to 215 Hz) of the cavity are considered in calculation. The dashed black curve is simulated with the modal method where only the first 9 cavity modes (i.e. cavity mode with cut-off frequency f_{m_n} below 100 Hz) are taken into account. Two notes have to be made:

- Curves computed with the modal method tend to the curve computed by the direct method (exact solution) when the number of acoustic modes considered in calculation increases. This is in agreement with expectations.
- The gain on the sound reduction index R computed by cancelling a great number of evanescent modes (dashed black curve) in the air cavity is largely higher than the gain computed by considering all evanescent modes (black curve).

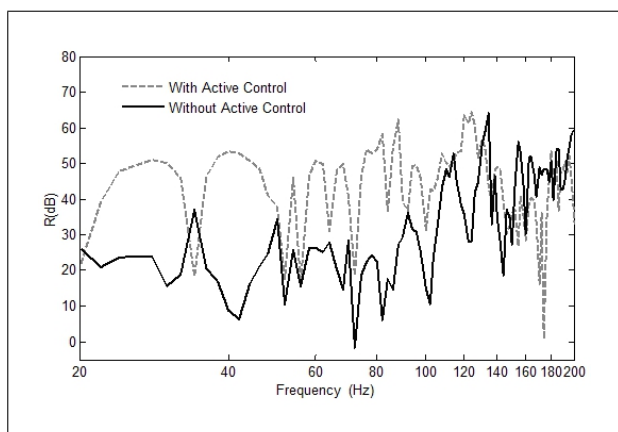


Figure 6. Sound reduction index $R(\text{dB})$ with and without active control simulated for 9 control channels.

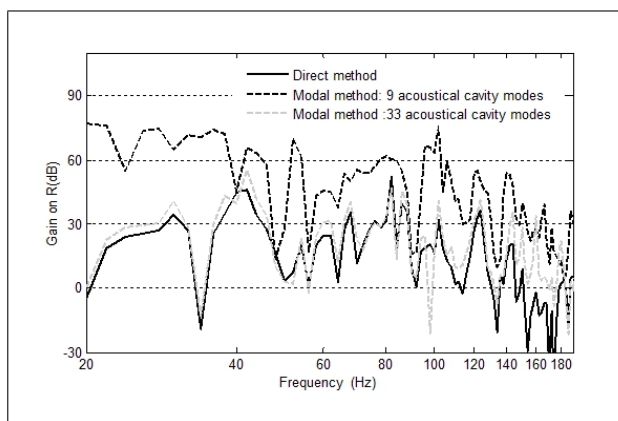


Figure 7. Gain on the sound reduction index R obtained by active control simulated for 9 control channels.

So, we can conclude that:

- Unlike for the passive case, the sound reduction index R is seriously affected by evanescent modes in the air cavity in the case of active noise control.
- Evanescent modes in the air cavity (which are generated by control sources and also by radiation and reflection of waves by the two gypsum plates) have a negative effect on the active control performance.

The negative effects of evanescent modes on the active control efficiency can be explained by the following facts:

- No acoustic energy can be transported by evanescent modes, their influence on the sound reduction index R is therefore negligible for the passive case. However, in the case of active control, evanescent modes greatly influence the acoustic pressure at the error microphones positions, due to control sources. Consequently, these evanescent mode have a negative influence on the active control performance.
- Even at very low frequencies, evanescent modes in the air cavity make the acoustic pressure distribution in the air cavity more complex (especially with respect to the x and y coordinates). As a result, the cancellation by active control of the acoustic pressure level at the 9 error microphones positions does not allow the cancellation of the pressure in the global microphones plane.

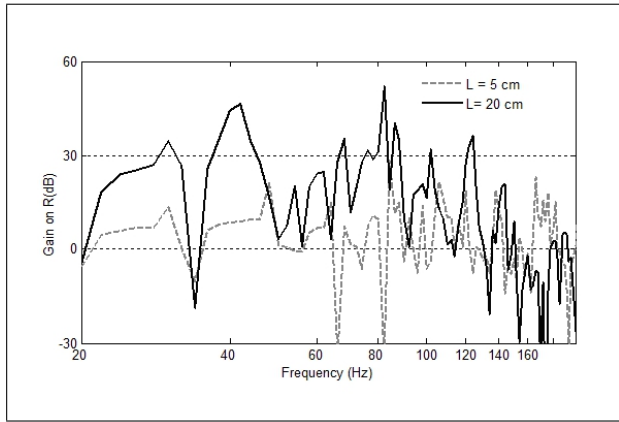


Figure 8. Gain on the sound reduction index R (dB) simulated for two different cavity thickness L of the double panel air cavity.

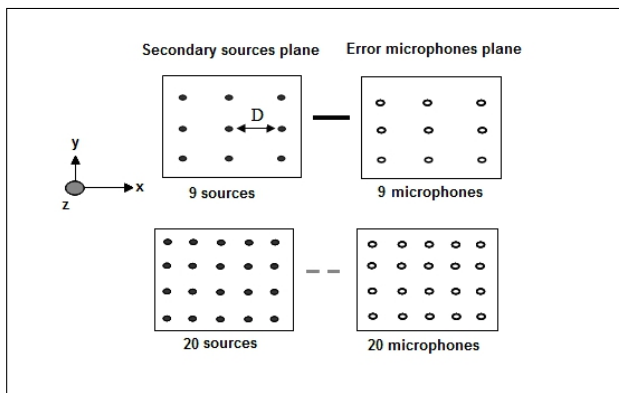


Figure 9. Schema of secondary sources plane at z_s and error microphones plane at z_m in the case of 9 and 20 active control channels.

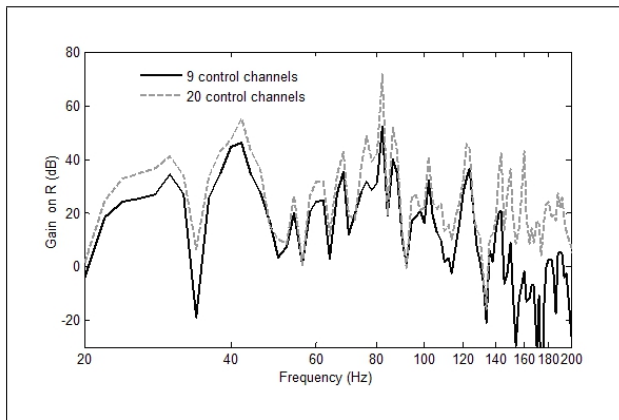


Figure 10. Gain on the sound reduction index R (dB) simulated for 9 and 20 noise control channels.

Negative effects of evanescent modes on the active control efficiency becomes very strong when the distance between error microphones and the gypsum two plates as well as secondary sources is reduced. This is indeed confirmed in Figure 8, since the gain on sound reduction index R simulated for 5 cm thick air cavity is smaller than that simulated for a 20 cm thick cavity. On the other hand, if error microphones and secondary sources are not positioned

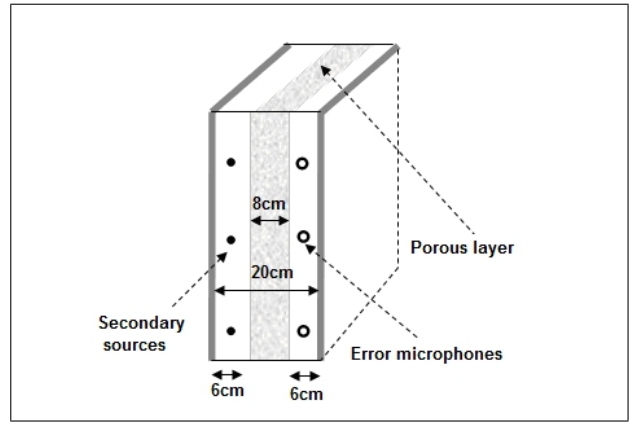


Figure 11. Schema of the double panel with a porous layer inserted in its cavity between secondary sources plane and error microphones plane.

exactly in front of each other as indicated in Figure 2, the distance d between sources and error microphones would be higher and negative effect of evanescent modes (only those created by secondary sources) will therefore be reduced. This can not significantly reduce the problem, because evanescent modes at microphones positions are not only generated by secondary sources but also by reflections and radiations of waves caused by the two plates.

In order to investigate the influence of the control channels number (number of secondary sources and microphones), Figure 10 presents a comparison between the gain on index R obtained by active control simulated with 9 and 20 control channels (see Figure 9 for distribution of control sources and error microphones). We can note that more than 8 dB gain is obtained on sound reduction index R in some frequency ranges when the number of control channels is increased from 9 to 20. Furthermore, with 20 control sources, the frequency band in which the gain on sound reduction index R remains positive is enlarged. This is in good agreement with equation (4) since for 20 control channels case, the distance D is equal to 0.6 m yielding a frequency f_{max} close to 290 Hz. However, those results show that in spite of increasing greatly the number of control channels, the active control efficiency has not been significantly improved at low frequencies. Indeed, due to the evanescent modes in double wall cavity, the gain on sound reduction index R obtained by increasing the number of control channels from 9 to 20 is not sufficiently important compared to the complexity of the control system that would have to be implemented in real life.

In order to bring a significant improvement on the active control efficiency, it is necessary to get rid of evanescent modes at error microphones positions. For doing so, an absorbent layer composed of porous material inserted between secondary sources and microphones planes (see Figure 11) could be a good solution. In fact, evanescent modes are more strongly attenuated in absorbent mediums such as porous materials than in the air fluid [2, 8, 19].

The porous material is modelled by Nastran software using an equivalent fluid approach. Expressions of the

speed of sound c_e in the porous layer and the associated density ρ_e used by the FE model are [2]

$$c_e(\omega) = \sqrt{\frac{K(\omega)}{\rho_e(\omega)}}, \quad (5)$$

$$\rho_e(\omega) = \alpha_\infty \rho_0 \left[1 - \frac{j\sigma\phi G(\omega)}{\alpha_\infty \rho_0 \omega} \right], \quad (6)$$

where

$$G(\omega) = \left(1 + \frac{j4\alpha_\infty^2 \eta \rho_0 \omega}{\sigma^2 \phi^2 \Lambda^2} \right)^{1/2}, \quad (7)$$

$$K(\omega) = \quad (8)$$

$$\frac{\gamma P_0}{\gamma - (\gamma - 1) \left[1 + \frac{8\eta}{j\Lambda'^2 \rho_0 Pr \omega} \left(1 + \frac{j\Lambda'^2 \rho_0 Pr \omega}{16\eta} \right)^{1/2} \right]^{-1}}.$$

K is the bulk modulus, parameters ϕ , α_∞ , σ , Λ and Λ' are porosity, tortuosity, flow resistivity and viscous and thermal characteristic length of the porous medium, respectively. $j = \sqrt{-1}$, ω , ρ_0 , Pr , γ and η are the angular frequency, air density, the ambient mean pressure, Prandtl number, air ratio of specific heats and air dynamic viscosity, respectively.

Note that for porous material, c_e and ρ_e are complex values and frequency dependent. The use of the modal method to solve FE motion equations is not appropriate and, frequency response analysis must be carried out using the direct method where motion equations are solved using complex arithmetic [18, 20].

Figure 12 represents the sound reduction index R of the double wall simulated for passive case (without active control) with and without a porous layer. The thickness of the porous layer is equal to 8 cm. Parameters used for modelling the porous layer are given in Table IV. With the porous layer, the sound reduction index R is globally in agreement with expectations. Indeed, the mass-spring-mass resonance frequency which is located around 45 Hz without porous layer, has been slightly shifted to lower frequencies when the porous layer is included in the double wall cavity.

Also, above 80 Hz, the index R simulated with the porous layer is generally higher than the one simulated without the porous layer. The curve of the index R has been considerably smoothed due to the increased damping in the system. These results concord with previous works [2, 4] since when the frequency increases, the acoustic energy is more dissipated by porous materials than by air.

The gain on the sound reduction index R obtained by active control simulated with and without the porous layer is plotted in Figure 13. The curve shows that with the porous layer, the noise active control is more efficient especially at low frequencies. In fact, more than 36 dB difference between the two curves (gain on sound reduction index R with and without the porous layer) has been noted for very low frequencies closed to 20 Hz. And, more than 20 dB difference for frequencies between 20 Hz and 70 Hz. Therefore, it can be concluded that the use of a porous

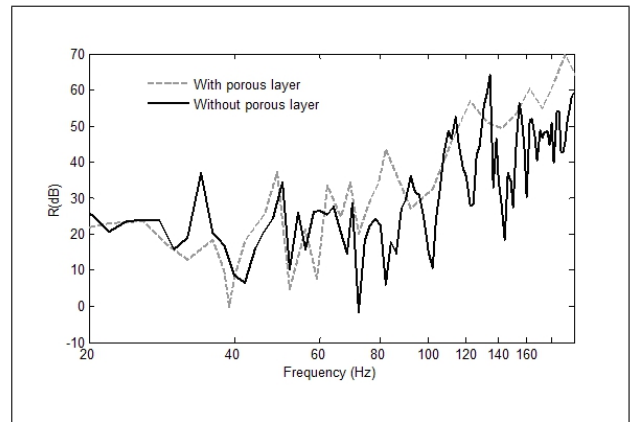


Figure 12. Sound reduction index R (dB) simulated for passive case (without active control) with and without the porous layer.

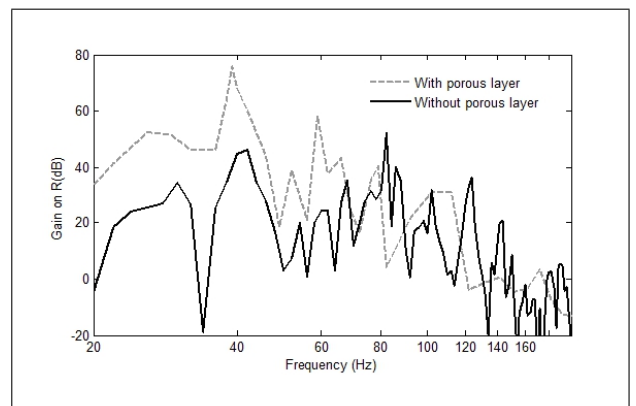


Figure 13. Gain on the sound reduction index R (dB) simulated with and without the porous layer.

Table IV. Parameters used for modelling the porous layer as an equivalent fluid.

Thickness	8 cm
Flow resistivity	$\sigma = 36000 \text{ Nm}^{-4}$
Porosity	$\phi = 0.95$
Tortuosity	$\alpha_\infty = 1.1$
Viscous characteristic length	$\Lambda = 150 \mu\text{m}$
Thermal characteristic length	$\Lambda = 220 \mu\text{m}$
Ambient mean pressure	$P_0 = 191325$
Prandtl number	$Pr = 0.702$
Air ratio of specific heats	$\gamma = 1.4$
Air dynamic viscosity	$\eta = 1.8 \cdot 10^{-5}$

layer between secondary sources and error microphones planes reduces significantly negative effect of evanescent modes and improves greatly the active control efficiency. However, the frequency f_{\max} defined by equation (4) has been shifted to lower frequencies below 120 Hz in the case of the porous layer. This is related to the difference between the speed of sound in air and the speed of sound in porous material (equation 5).

5. Conclusion

In this work, a simulation method for predicting the sound reduction index of a double wall including active control sources and porous layer in double wall cavity has been developed. Calculation steps have been described and effects of some parameters on active noise control efficiency have been simulated and discussed. Main conclusions of this work are:

- Evanescent modes in the double panel air cavity minimise seriously the active control efficiency at low frequencies even when the number of control channels is important. This is essentially due to the fact that evanescent modes greatly influence the acoustic pressure at the error microphones positions. This negative effect of evanescent modes becomes stronger when the air cavity thickness is decreased.
- The use of an absorbent layer made of porous material, placed between secondary sources plane and error microphone plane, reduces evanescent modes influence at error microphones positions and improves significantly the active control performance at low frequencies.

In future works, the measurement of the sound reduction index of double walls equipped with active noise control system will be carried out and effects of other factors such as control sources directivity (monopoles, dipoles, or others) and frequency response of realistic secondary sources will be investigated.

Appendix

Assuming that lateral walls of the double panel cavity are rigid. Then, the acoustic pressure distribution in the double panel air cavity can be written in terms of transverse modes in rectangular coordinates system (x, y, z) as [21]

$$P(x, y, z, t) = \sum_{m=-\infty}^{+\infty} \sum_{n=-\infty}^{+\infty} P_{mn}(z) \psi_{mn}(x, y) e^{-j\omega t}. \quad (A1)$$

The eigenfunctions ψ_{mn} are given by [8, 10, 11]

$$\psi_{mn}(x, y) = \cos(\pi m/L_x x) \cos(\pi n/L_y y). \quad (A2)$$

The modal pressure in the air cavity in a cross section located at axial coordinate z is

$$P_{mn}(z) = P_{mn}^+(0) e^{+jk_{mn}z} + P_{mn}^-(0) e^{-jk_{mn}z}, \quad (A3)$$

where

$$k_{mn} = \frac{2\pi}{c_0} \sqrt{f^2 - f_{mn}^2}, \quad (A4)$$

$$f_{mn} = \frac{c_0}{2} \sqrt{(m/L_x)^2 + (n/L_y)^2}. \quad (A5)$$

P_{mn}^+ and P_{mn}^- are respectively the complex amplitudes of modes travelling in the positive and negative z directions inside the double panel air cavity at z axis origin ($z = 0$). (Here, z axis origin is located at $z_e + h$, where h is the plate thickness as shown in Figure 2). Indices m and n correspond to the cavity modes index in the x and y directions respectively. The cavity dimensions in the x and y

directions are denoted L_x and L_y respectively. The modal wave number in the z -direction is represented by k_{mn} . f_{mn} is the cut-off frequency of mode (m, n) (or eigenfrequency of transverse modes).

According to the frequency f , two cases have to be distinguished:

- If $f > f_{mn}$, k_{mn} is a real value and (m, n) is a propagating mode.
- If $f < f_{mn}$, k_{mn} is an imaginary number and the mode (m, n) is called evanescent. In this case, we have

$$k_{mn} = \pm j |k_{mn}| = \pm j \frac{2\pi}{c_0} \sqrt{|f^2 - f_{mn}^2|}. \quad (A6)$$

Only converging solutions have physical meaning. The modal pressure $P_{mn}(z)$ becomes

$$P_{mn}(z) = P_{mn}^+(z=0) e^{-|k_{mn}|z} + P_{mn}^-(z=0) e^{+|k_{mn}|z}. \quad (A7)$$

The z -direction component of acoustic intensity of mode (m, n) [11] is defined by

$$I_{z,mn} = 1/2 \text{Re} \{ P_{mn} V_{z,mn}^* \}, \quad (A8)$$

where the modal coefficient of the acoustic particle velocity in the z -direction $V_{z,mn}$ is given by

$$V_{z,mn}(z) = \frac{k_{mn}}{Z_0 k} (P_{mn}^+ e^{+jk_{mn}z} - P_{mn}^- e^{-jk_{mn}z}). \quad (A9)$$

With Z_0 the air impedance (equals $\rho_0 c_0$) and k the wave number in cavity.

Combining equations (A3), (A8) and (A9) yields

$$I_{z,mn} = \frac{1}{2} \text{Re} \left\{ \frac{k_{mn}}{\rho_0 c_0 k} (|P_{mn}^+|^2 - |P_{mn}^-|^2) \right\}. \quad (A10)$$

When the mode (m, n) is evanescent, k_{mn} is an imaginary complex number (equation A6), the acoustic intensity $I_{z,mn}$ is then equal to zero. Accordingly, the acoustic energy can not be transported by evanescent modes.

Acknowledgement

The authors thank the support of the project PARABAS (Parois Acoustiques Basses Fréquences: ANR-06-BLAN-0081-01).

References

- [1] C. Hopkins: Sound insulation. Butterworth-Heinemann, 2007.
- [2] J. F. Allard: Propagation of sound in porous media. Modelling sound absorbing materials. Elsevier applied sciences, 1993.
- [3] P. Nelson, S. J. Elliott: Active control of sound. Academic Press Limited, London, 1992.
- [4] Y. Hu, A. Sitel, M.-A. Galland, K. Chen: A plane wave study for improving acoustical performance of double wall systems using an active passive method. Noise Control Eng. J. **57** (2009) 193–202.
- [5] P. Sas, C. Bao, F. Augusztinovicz, W. Desmet: Active control of sound transmission through a double panel partition. J. Sound Vib. **180** (1995) 609–625.

- [6] J. P. Carneal, C. R. Fuller: An analytical and experimental investigation of active structural control of noise transmission through double panel system. *J. Sound Vib.* **272** (2004).
- [7] T. Sugimoto, K. Ono, A. Ando, K. Kurozumi, A. Hara, Y. Morita, A. Miura: PVDF-driven flexible and transparent loudspeaker. *Applied Acoustics* **70** (2009) 1021–1028.
- [8] C. Lesueur: Rayonnement acoustique des structure. Eyrolles, Paris, 1988.
- [9] A. Sitel: Méthodes de mesure des matrices acoustiques des discontinuités à un ou à deux ports en présence des modes élevés. PHD Dissertation. University of Technology of Compiègne, 2005.
- [10] A. Sitel, J.-M. Ville, F. Foucart: Multiload procedure for measurement of acoustic scattering matrix of a duct discontinuity for higher order modes propagation conditions. *J. Acoust. Soc. Am.* **120** (2006) 2478–2490.
- [11] A. Sitel, J. M. Ville, F. Foucart: An experimental facility of acoustic transmission matrix and acoustic power dissipation of duct discontinuity in higher order modes propagation conditions. *Acta Acustica united with Acustica* **88** (2002) 924–933.
- [12] P. Jean, P., J.-F. Rondeau: A simple decoupled modal calculation of sound transmission between volumes. *Acta Acustica united with Acustica* **88** (2002) 924–933.
- [13] P. Jean, H. Siwiak, G. Joubert: A decoupled vibro-acoustic development of fem: application to laboratory modelling. *Building Acoustics* **13** (2006) 83–8.
- [14] P. Jean, J. Roland: Application of the green ray integral method (GRIM) to sound transmission problem. *Building Acoustics* **8** (2001) 139–156.
- [15] P. Jean: A combined use of geometrical and BEM methods for vibro-acoustic problems. 6th ICSV, Copenhagen, 5-8 July, 1999.
- [16] E. Premat, Y. Gabillet: A new boundary-element method for predicting outdoor sound propagation and application to the case of a sound barrier in the presence of downward refraction. *J. Acoust. Soc. Am.* **108** (2000) 2775–2783.
- [17] P. Jean, J. Roland: A model for the calculation of noise transmission inside dwellings. Application to aircraft noise. *Applied Acoustics* **65** (2004) 861–882.
- [18] MSC Nastran 2007 r1 Release Guide.
- [19] M. C. Munjal: Acoustics of ducts and mufflers. John Wiley, New York, 1987.
- [20] J. Wandinger: Possible implementations of porous absorbers in nastran. MSC internal memo, April 2006.
- [21] T. Schultz, I. L. N. Cattafesta, M. Sheplak: Modal decomposition method for acoustic impedance testing in square ducts. *J. Acoust. Soc. Am.* **120** (2006) 3750–3758.